Inorg. Chem. **2006**, *45*, 3014–3022

Linear Polypseudorotaxanes Possessing Many Metal Centers Constructed from Inclusion Complexes of α-, β-, and γ-Cyclodextrins with 4,4′-Dipyridine

Ying-Wei Yang, Yong Chen, and Yu Liu*

Department of Chemistry, State Key Laboratory of Elemento-Organic Chemistry, Nankai University, Tianjin 300071, P. R. China

Received January 24, 2006

Three cyclodextrin-based complexes, **1**–**3**, bearing external coordination sites for metal cations were prepared in satisfactory yields (over 50%) by reactions of α-, β-, and γ-cyclodextrins with 4,4′-dipyridine in aqueous solutions. Subsequently, these inclusion complexes were further assembled to form linear polypseudorotaxanes **4**–**6** through the coordination linkage of Ni(II) or Cu(II) ions, and their assembly behaviors were comprehensively investigated in both solutions and the solid state by means of ^{1}H NMR, FT-IR, UV–vis spectroscopy, conductivity titration, powder X-ray diffraction patterning, thermogravimetric and differential thermal analysis, scanning electron microscopy, scanning tunneling microscopy, and transmission electron microscopy. The results showed that these polypseudorotaxanes existed as individual linear arrays at a low concentration but tended to form polymeric rodlike fibers at a relatively high concentration. Significantly, the volume of the cyclodextrin cavity used not only determined the inclusion complexation stoichiometry between cyclodextrin and 4,4′-dipyridine but also predominated the morphology of resulting polypseudorotaxanes.

Introduction

Macrocyclic oligosaccharides called cyclodextrins (α-, β-, and γ-CDs) can form stable inclusion complexes with various substrate molecules, in which target molecules are included in the hydrophobic cavities of CDs through host−guest complexation.[1−4] On the basis of this simple inclusion complexation of CDs (receptor) and target molecules (substrate), many nanometer-sized supramolecular aggregates were constructed and exhibited a great deal of potential to serve as molecular devices and machines, as well as functional materials.[3−5] For example, Harada et al. prepared tens of CD-based polypseudorotaxanes and polyrotaxanes by threading many CD units onto a polymer chain[6] and then extended them to molecular tubes through the covalent cross-linking of adjacent CD units in a polyrotaxane.[7] Stoddart et al. prepared some polyrotaxanes and reviewed a number of CD-containing aggregates formed by host−guest complexation, which exhibited significant chemical and biological functions.[8] Li and McGown reported that β- and γ-CDs could be constructed to molecular nanometer tubes using diphenylhexatrienes as linkers.[9] Anderson et al. and Cacialli et al. reported that conjugated polyrotaxanes threading α- or β-CDs could form insulated molecular wires.[10] In addition, molecular semiconductors and nanoengineered devices at a supramolecular level were also prepared by threading a

* Author to whom correspondence should be addressed. Tel.: +86-022-23503625. E-mail: yuliu@nankai.edu.cn.

(1) (a) Szejtli, J.; Osa, T. In *Comprehensive Supramolecular Chemistry*; Atwood, J. L., Davies, J. E., MacNicol, D. D., Vögtle, F., Eds.; Pergamon/Elsevier: Oxford, U. K., 1996; Vol. 3. (b) Easton, C. J.; Lincoln, S. F. *Modified Cyclodextrins, Scaffolds and Templates for Supramolecular Chemistry*; Imperial College Press: London, U. K., 1999. (c) Breslow, R.; Dong, S. D. *Chem. Rev.* **1998**, *98*, 1997.
(2) Wenz, G. *Angew. Chem., Int. Ed. Engl.* **1994**, *33*, 803.
(3) (a) Nepogodiev, S. A.; Stoddart, J. F. *Chem. Rev.* **1998**, *98*, 1959. (b) Raymo, F. M.; Stoddart, J. F. *Chem. Rev.* **1999**, *99*, 1643.
(4) Harada, A. *Acc. Chem. Res.* **2001**, *34*, 456.
(5) (a) Hong, B. H.; Bae, S. C.; Lee, C.-W.; Jeong, S.; Kim, K. S. *Science* **2001**, *294*, 348. (b) Bong, D. T.; Clark, T. D.; Granja, J. R.; Ghadiri, M. R. *Angew. Chem., Int. Ed.* **2001**, *40*, 988. (c) Qu, D. H.; Wang, G. C.; Ren, J.; Tian, H. *Org. Lett.* **2004**, *6*, 2085. (d) Wang, Q. C.; Qu, D. H.; Ren, J.; Chen, K. C.; Tian, H. *Angew. Chem., Int. Ed.* **2004**, *43*, 2661.
(6) (a) Harada, A.; Kamachi, M. *Macromolecules* **1990**, *23*, 2821. (b) Harada, A.; Li, J.; Kamachi, M. *Macromolecules* **1993**, *26*, 5698. (c) Harada, A.; Li, J.; Nakamitsu, T.; Kamachi, M. *J. Org. Chem.* **1993**, *58*, 237. (d) Harada, A.; Okada, M.; Li, J.; Kamachi, M. *Macromolecules* **1995**, *28*, 8406. (e) Okada, M.; Harada, A. *Org. Lett.* **2004**, *6*, 361. (f) Miyauchi, M.; Harada, A. *J. Am. Chem. Soc.* **2004**, *126*, 11418. (g) Okumura, H.; Kawaguchi, Y.; Harada, A. *Macromolecules* **2001**, *34*, 6338.
(7) (a) Harada, A.; Li, J.; Kamachi, M. *Nature* **1992**, *356*, 325. (b) Harada, A.; Li, J.; Kamachi, M. *Nature* **1993**, *364*, 516.

10.1021/ic0601438 CCC: $33.50
Published on Web 03/08/2006

Scheme 1

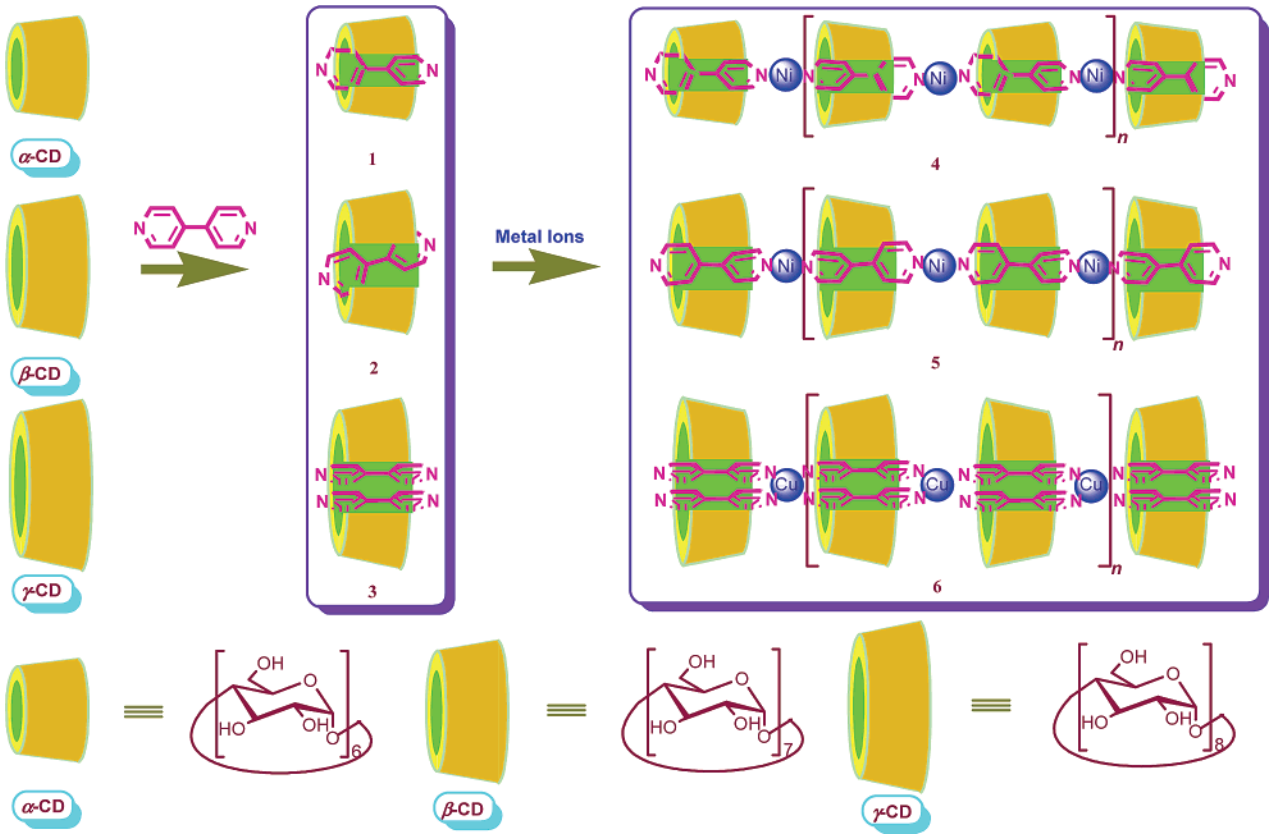

charge-transport macromolecule.[11] In recent years, we presented some significant results on the construction of nanometer-sized supramolecular aggregates, for example, polypseudorotaxanes and bis(polypseudorotaxane)s as nanotubes, heterogeneous aggregates formed by bis(CD)s and bulk organic molecules as nanowires, nanometer-scale functional materials constructed from small polyrotaxanes with cyclodextrins as stoppers, CD-modified gold nanoparticles as captors for fullerenes, and luminescent or electrochemical active supramolecular links.[12] These works efficiently applied some generally used methods for the construction of CD-based aggregates. These methods include the self-assembly of CD derivatives,[12d] the threading of CDs onto a polymer chain,[12a,b,e,i,j] the noncovalent linkage through the 2:1 inclusion complexation between CD cavities and bulk organic molecules,[12c,g,h,k,m] the direct polycondensation reaction between CD/dialdehyde and CD/diamine complexes,[12f] and the complexation of the cyclodextrin−dipyridine complex and metal ions.[12l] However, the construction methodology of highly ordered CD-based aggregates by the coordination linkage of metal ions is still rare, to the best of our knowledge. In our previous communication, we reported an uncommon polypseudorotaxane prepared by β-CD/4,4′-dipyridine complexes and Ni(II) ions.[13a] In the present work, we wish to extend our works by comprehensively investigating the inclusion complexation behaviors of α-, β-, and γ-CDs with 4,4′-dipyridine (DPD) and the assembly behaviors of resulting CD/DPD complexes through the coordination linkage of metal cations in both solutions and the solid state (Scheme 1). It is our special interest to explore the structures and stabilities of CD/DPD complexes and their

(8) (a) Nelson, A.; Stoddart, J. F. *Org. Lett.* **2003**, *5*, 3783. (b) Tseng, H. R.; Vignon, S. A.; Stoddart, J. F. *Angew. Chem., Int. Ed.* **2003**, *42*, 1491. (c) Stoddart, J. F. *Chem.—Eur. J.* **2003**, *9*, 2982. (d) Horn, M.; Ihringer, J.; Glink, P. T.; Stoddart, J. F. *Chem.—Eur. J.* **2003**, *9*, 4046. (e) Chiu, S.-H.; Elizarov, A. M.; Glink, P. T.; Stoddart, J. F. *Org. Lett.* **2002**, *4*, 3561. (f) Collier, C. P.; Jeppesen, J. O.; Luo, Y.; Perkins, J.; Wong, E. W.; Heath, J. R.; Stoddart, J. F. *J. Am. Chem. Soc.* **2001**, *123*, 12632. (g) Nepogodiev, S. A.; Stoddart, J. F. *Chem. Rev.* **1998**, *98*, 1959.

(9) Li, G.; McGown, L. B. *Science* **1994**, *264*, 249.

(10) (a) Taylor, P. N.; O'Connell, M. J.; McNeill, L. A.; Hall, M. J.; Aplin, R. T.; Anderson, H. L. *Angew. Chem., Int. Ed.* **2000**, *39*, 3456. (b) Cacialli, F. *Nat. Mater.* **2002**, *1*, 160.

(11) (a) Zhu, S. S.; Swager, T. M. *J. Am. Chem. Soc.* **1997**, *119*, 12568. (b) Maclachlan, M. J.; Rose, A.; Swager, T. M. *J. Am. Chem. Soc.* **2001**, *123*, 9180. (c) Shukla, A. D.; Bajaj, H. C.; Das, A. *Angew. Chem., Int. Ed.* **2001**, *40*, 446. (d) Lee, J. W.; Samal, S.; Selvapalam, N.; Kim, H.-J.; Kim, K. *Acc. Chem. Res.* **2003**, *36*, 621. (e) Ong, W.; Gomez-Kaifer, M.; Kaifer, A. E. *Org. Lett.* **2002**, *4*, 1791.

(12) (a) Liu, Y.; You, C.-C.; Zhang, H.-Y.; Kang, S.-Z.; Zhu, C.-F.; Wang, C. *Nano Lett.* **2001**, *1*, 613. (b) Liu, Y.; Li, L.; Zhang, H.-Y.; Zhao, Y.-L.; Wu, X. *Macromolecules* **2002**, *35*, 9934. (c) Liu, Y.; Li, L.; Fan, Z.; Zhang, H.-Y.; Wu, X.; Liu, S.-X.; Guan, X.-D. *Nano Lett.* **2002**, *2*, 257. (d) Liu, Y.; Fan, Z.; Zhang, H.-Y.; Yang, Y.-W.; Ding, F.; Liu, S.-X.; Wu, X.; Wada, T.; Inoue, Y. *J. Org. Chem.* **2003**, *68*, 8345. (e) Liu, Y.; Song, Y.; Wang, H.; Zhang, H.-Y.; Li, X.-Q. *Macromolecules* **2004**, *37*, 6370. (f) Liu, Y.; Zhao, Y.-L.; Li, X.-Y.; Liang, P.; Zhang, X.-Z.; Xu, J.-J. *Macromolecules* **2004**, *37*, 6362. (g) Liu, Y.; Wang, H.; Liang, P.; Zhang, H.-Y. *Angew. Chem., Int. Ed.* **2004**, *43*, 2690. (h) Liu, Y.; Wang, H.; Zhang, H.-Y.; Liang, P. *Chem. Commun.* **2004**, 2266. (i) Liu, Y.; Wang, H.; Chen, Y.; Ke, C.-F.; Liu, M. *J. Am. Chem. Soc.* **2005**, *127*, 657. (j) Liu, Y.; Yang, Y.-W.; Chen, Y.; Zou, H.-X. *Macromolecules* **2005**, *38*, 5838. (k) Liu, Y.; Yang, Y.-W.; Chen, Y. *Chem. Commun.* **2005**, 4208. (l) Liu, Y.; Song, S.-H.; Chen, Y.; Zhao, Y.-L.; Yang, Y.-W. *Chem. Commun.* **2005**, 1702. (m) Liu, Y.; Liang, P.; Chen, Y.; Zhang, Y.-M.; Zheng, J.-Y.; Yue, H. *Macromolecules* **2005**, *38*, 9095.

influences on the morphology of resulting polypseudorotaxanes. These investigations may open new access to the design and construction of polymeric supramolecular aggregates containing many chiral (e.g., CD) or achiral (e.g., calixarene, crown ether, and cucurbituril) macromolecules and metal units and will serve our further understanding of this quite significant, but less investigated, area of supramolecular chemistry.

Experimental

General. α-, β-, and γ-CDs and 4,4′-dipyridine were purchased from Sigma. ^{1}H NMR experiments were carried out in deuterium oxide at 298.2 ± 0.1 K on a Bruker AV600 spectrometer. Tetramethylsilane was used as a reference, and no correction was made for susceptibility of the capillary. For the rotating frame nuclear Overhauser effect spectroscopy (ROESY), a Bruker standard sequence with water suppression (roesyphpr) was necessary to remove the signal of residual HOD and to be able to observe weak intermolecular NOE interactions. The data consisted of eight scans collected over 2048 complex points and for a spectral width of 6127 Hz. A mixing time of 200 ms, a repetition delay of 1.5 s, an acquisition time of 0.167 s, and a 90° pulse width of 7.95 μs at a −3 dB power attenuation were used. The data were zero-filled to 1024 × 1024 points and processed by applying a π/2 shifted Q-sine window in both dimensions. Small cross-peaks were neglected when their magnitude was close to that of noise. Circular dichroism and UV−vis spectra were recorded in a conventional quartz cell (light path, 10 mm) on a JASCO J-715S spectropolarimeter or a Shimadzu UV-2401PC spectrophotometer equipped with a PTC-348WI temperature controller to keep the temperature at 25 °C. FT-IR spectra were obtained on a Bio-Rad FTS 135 FT-IR spectroscopy device. The sample was mixed with KBr and compressed as a disk; 16 scans were signal-averaged at a resolution of 8 cm^{-1}. Scanning electron microscopy (SEM) experiments were performed on a HITACHI S-3500N scanning electron microscope. Scanning tunneling microscopy (STM) experiments were performed by using an easyScan STM System E 230V (Nanosurf, Switzerland) with a Pt−Ir tip and were carried out with a sample bias voltage of +100 mV. All images were recorded in the constant-current mode. An aqueous solution of the sample was prepared at a dilute concentration of 5 × 10^{-6} M and dripped onto a freshly prepared, highly ordered pyrolytic graphite surface at room temperature. The sample was then dried in vacuo for 2 h. All measures were performed in the air at room temperature. Transmission electron microscopy (TEM) experiments were performed using a Philips Tacnai G^2 20 S-TWIN microscope operating at 200 keV. TEM samples were prepared by depositing a drop of the suspension onto a holey carbon grid or by placing a drop of the solution onto a carbon-coated copper grid. Thermogravimetric (TG) and differential thermal analyses (DTA) were performed with a RIGAKU Standard-type spectrometer. Samples were heated at 10 °C/min from room temperature to 700 °C in a dynamic nitrogen atmosphere (flow rate = 70 mL/min). Powder X-ray patterns were obtained using a Rigaku D/max-2500 diffractometer with Cu Kα radiation (40 kV and 100 mA). Powder samples were mounted on a sample holder and scanned with a step size of 2θ = 0.02° between 2θ = 3° and 60°.

Complex 1. A mixture of α-CD (1 mmol) and 4,4′-dipyridine (1 mmol) in 20 mL of H_2O was allowed to react under ultrasonic vibrations at room temperature for 5 min and then was stirred at 30 °C for 5 h. The precipitate formed was filtrated to give a white powder. The crude product was washed with a small amount of ethanol and then recrystallized by water to give **1** in a yield of 66%. ^{1}H NMR (D_2O, TMS, ppm): δ 3.49−3.55 (m, 12H), 3.75−3.86 (m, 24H), 4.96 (d, 6H), 7.69 (d, 4H, meta protons of DPD), 8.60 (d, 4H, ortho protons of DPD). Elem Anal. Calcd for $C_{46}H_{68}O_{30}N_2 \cdot 2H_2O$: C, 47.42; H, 6.23; N, 2.40%. Found: C, 47.38; H, 6.40; N, 2.57%. FT-IR (KBr): ν_{max}/cm^{-1} 3347, 2930, 2152, 1650, 1596, 1537, 1456, 1416, 1329, 1295, 1241, 1152, 1079, 1035, 947, 853, 805, 754, 704, 611, 575, 528. UV−vis: λ_{max} (ε) 239 nm (21 050 mol^{-1} dm^3 cm^{-1}).

Complex 2. The β-CD/DPD complex **2** was prepared according to our previous report.[13] Yield: 78%. ^{1}H NMR (D_2O, TMS, ppm): δ 3.37−3.69 (m, 42H), 4.88−4.90 (d, 7H), 7.53−7.55 (d, 4H), 8.52−8.54 ppm (d, 4H). Elem Anal. Calcd for $C_{52}H_{78}O_{35}N_2 \cdot 7H_2O$: C, 44.07; H, 6.54; N, 1.98%. Found: C, 43.73; H, 6.04; N, 2.37%. FT-IR (KBr): ν_{max}/cm^{-1} 3341, 2929, 1595, 1534, 1414, 1365, 1332, 1299, 1241, 1155, 1080, 1032, 944, 851, 805, 756, 611, 578, 528. UV−vis: λ_{max} (ε) 239 nm (17 400 mol^{-1} dm^3 cm^{-1}).

Complex 3. γ-CD (0.25 mmol) and 4,4′-dipyridine (0.51 mmol) were dissolved in 6 mL of H_2O, and the reaction mixture was stirred at 35 °C for 16 h and then maintained at 4 °C for 5 days. The precipitate formed was filtrated to give a white powder, which was washed with a small amount of ethanol and water to give **3** in 50% yield. ^{1}H NMR (D_2O, TMS, ppm): δ 3.35−3.67 (m, 48H), 4.90 (d, 8H), 7.51 (d, 8H, meta protons of DPD), 8.42 (d, 8H, ortho protons of DPD). Elem Anal. Calcd for $C_{68}H_{96}O_{40}N_4 \cdot 4H_2O$: C, 48.57; H, 6.23; N, 3.33%. Found: C, 48.90; H, 6.40; N, 3.63%. FT-IR (KBr): ν_{max}/cm^{-1} 3346, 2925, 1650, 1595, 1536, 1486, 1413, 1335, 1218, 1155, 1081, 1028, 939, 853, 805, 758, 705, 613, 583, 527. UV−vis: λ_{max} (ε) 239 nm (18 600 mol^{-1}dm^3 cm^{-1}).

Polypseudorotaxane 4. An aqueous solution (10 mL) containing $NiCl_2 \cdot 6H_2O$ (0.1 mmol) was added dropwise to an aqueous solution (20 mL) of **1** (0.1 mmol). The resultant mixture was stirred at 40 °C for 7h. The solvent was concentrated under reduced pressure, and the precipitate formed was collected by filtration to give a green powder. The crude product was recrystallized by water and dried in vacuo to give **4** in a yield of 40%. ^{1}H NMR (D_2O, TMS, ppm): δ 3.27−4.08 (m, br, 36H), 4.96 (overlapped with HDO, 6H), 7.73 (br, 4H), 8.57 (br, 4H). Elem Anal. Calcd for $(C_{46}H_{68}O_{30}N_2NiCl_2 \cdot 8H_2O)_n$: C, 39.39; H, 6.04; N, 2.00%. Found: C, 39.50; H, 6.30; N, 2.17%. FT-IR (KBr): ν_{max}/cm^{-1} 3385, 3061, 2930, 1942, 1607, 1536, 1491, 1414, 1330, 1220, 1153, 1079, 1046, 945, 855, 808, 728, 635, 568. UV−vis: λ_{max} (ε) 242 nm (27 850 mol^{-1} dm^3 cm^{-1}), 348 nm (250 mol^{-1} dm^3 cm^{-1}).

Polypseudorotaxane 5. The polypseudorotaxane **5** was prepared according to our previous report.[13] Yield: 35%. ^{1}H NMR (D_2O, TMS, ppm): 3.39−3.81 (m, 42H), 4.90−4.91 (d, 7H), 7.62−7.64 (d, 4H), 8.50−8.52 (d, 4H). Elem Anal. Calcd for $(C_{52}H_{78}O_{35}N_2NiCl_2 \cdot 10H_2O)_n$: C, 39.01; H, 6.17; N, 1.75%. Found: C, 39.27; H, 6.00; N, 1.51%. FT-IR (KBr): ν_{max}/cm^{-1} 3358, 2930, 1608, 1535, 1491, 1415, 1332, 1221, 1156, 1079, 1031, 945, 855, 809, 756, 707, 577, 531. UV−vis: λ_{max} (ε) 239 nm (27 500 mol^{-1} dm^3 cm^{-1}), 358 nm (700 mol^{-1} dm^3 cm^{-1}).

Polypseudorotaxane 6. An aqueous solution (5 mL) of $CuCl_2 \cdot 6H_2O$ (0.1 mmol) was added dropwise to an aqueous solution (15 mL) of **3** (0.1 mmol). The resultant mixture was then stirred at 40 °C for 10 h and then allowed to stay at 4 °C in a refrigerator for 2 days. The precipitate formed was collected by centrifugation to give a blue powder. The crude product was recrystallized by water and dried in vacuo to give pure sample **6** (yield 30%). Elem Anal. Calcd for $(C_{68}H_{96}O_{40}N_4CuCl_2 \cdot 10H_2O)_n$: C, 42.45; H, 6.08; N,

(13) (a) Liu, Y.; Zhao, Y.-L.; Zhang, H.-Y.; Song, H.-B. *Angew. Chem., Int. Ed.* **2003**, *42*, 3260. (b) Liu, Y.; Zhao, Y.-L.; Zhang, H.-Y.; Yang, E.-C.; Guan, X.-D. *J. Org. Chem.* **2004**, *69*, 3383.

2.91%. Found: C, 42.36; H, 6.33; N, 3.03%. FT-IR (KBr): ν_{max}/cm^{-1} 3372, 3037, 2920, 1944, 1608, 1536, 1492, 1417, 1329, 1220, 1156, 1082, 1017, 854, 812, 728, 645, 566, 507. UV−vis: λ_{max} (ϵ) 239 nm (50 950 mol^{-1} dm^3 cm^{-1}), 351 nm (350 mol^{-1} dm^3 cm^{-1}).

Results and Discussion

Synthesis. Inclusion complexes **1**−**3** were synthesized in more than 50% yields by reactions of α-, *β*-, and *γ*-CDs with DPD. Because CDs are soluble, while CD/DPD complexes are less soluble in water, the resulting CD/DPD complex could be easily separated from the reaction system as a precipitate. Besides the elemental analyses data, ^{1}H NMR and FT-IR data also confirmed the formation of CD/DPD complexes. In general, the inclusion complexation of a guest molecule into a CD cavity will lead to appreciable changes of chemical shift values of guest protons.[14−16] In a preliminary work, we observed a change in the chemical shift values of all DPD protons in the presence of *β*-CD relative to a free DPD molecule: NMR signals of meta protons shifted upfield (ca. 0.02 ppm), and NMR signals of ortho protons shifted downfield (ca. 0.09 ppm).[13] Under identical conditions, similar phenomena were also observed in the case of complex **1** or **3**. For α-CD/DPD complex **1**, NMR signals of DPD's meta protons and ortho protons shifted downfield by 0.13 and 0.16 ppm, respectively, relative to a free DPD molecule. For *γ*-CD/DPD complex **3**, NMR signals of these protons shifted upfield by 0.05 (meta protons) and 0.02 ppm (ortho protons). Moreover, a comparison of the integral area of proton peaks indicated that the ratio among DPD's aromatic protons (a molecule of DPD contains eight aromatic protons), CD's H-1 protons (a molecule of α-, *β*-, or *γ*-CD contains six, seven, or eight H-1 protons, respectively), and CD's H-2/H-3/H-4/H-5/H-6 protons (a molecule of α-, *β*-, or *γ*-CD contains 36, 42, and 48 H-2/H-3/H-4/H-5/H-6 protons, respectively) was 8:6:36, 8:7:42, and 16:8:48 for complexes **1**−**3**, respectively. This result indicated that the inclusion complexation stoichiometry between CD and DPD was 1:1 for **1**, 1:1 for **2**, and 1:2 for **3**, which was consistent with the elemental analyses results. In addition, all of the FT-IR spectra of **1**−**3** showed typical stretching vibration bands at ca. 1595 cm^{-1} assigned to C═N groups in the DPD. These results jointly demonstrated that inclusion complexes were formed between CDs and DPD.

Further additions of metal cations to solutions of complexes **1**−**3** gave metallo-linked polypseudorotaxanes **4**−**6** in moderate yields (30−40%) as precipitates, which could be easily separated by filtration and purified by recrystallization. For stoichiometric 1:1 complexes **1** and **2**, the Ni(II) ion was employed because its octahedral coordination geometry could enable a linear arrangement of the resulting polypseudorotaxane. For the same purpose, the Cu(II) ion was selected for the stoichiometric 1:2 complex **3** because of its square-planar coordination geometry. Besides elemental analyses data and obviously decreased water solubilities of **4**−**6** as compared with those of their precursors **1**−**3**, some other experimental results also confirmed the formation of polypseudorotaxanes **4**−**6**. For example, the UV−vis spectra of polypseudorotaxanes **4**−**6** showed obvious enhancements on intensities of absorption peaks around 239 nm ($\Delta\epsilon$ = 6800−32 350 mol^{-1} dm^3 cm^{-1}) as compared to those of their corresponding precursors **1**−**3**, along with the appearance of ligand-to-metal charge-transfer bands at ca. 345−360 nm (ϵ = 250−700 mol^{-1} dm^3 cm^{-1}). In FT-IR spectra of polypseudorotaxanes **4**−**6**, vibration bands assigned to C═N groups in DPD shifted to the high wavenumber region as compared with those of uncoordinated precursors **1**−**3** (for **4**, from 1596 to 1607 cm^{-1}; for **5**, from 1595 to 1608 cm^{-1}; for **6**, from 1595 to 1608 cm^{-1}). In addition, ^{1}H NMR signals assigned to DPD's meta protons in **4** and **5** respectively deshielded by ca. 0.04 and 0.09 ppm, while the ortho protons did so by ca. 0.03 and 0.02 ppm, upon introduction of the Ni(II) ion. These experimental results jointly verified the efficient coordination of metal cations with CD/DPD complexes. Somewhat unfortunately, because of the paramagnetic disturbance of copper(II), the ^{1}H NMR spectrum of polypseudorotaxane **6** was unable to be measured. It is noteworthy that we tried to prepare Cu(II)-coordinating species of CD/DPD complexes as reference compounds, but only *γ*-CD/DPD could produce the desired Cu(II) complex. For α-CD/DPD and *β*-CD/DPD complexes, the included DPD components would dissociate with CD cavities upon coordinating Cu(II) and thus give the products that were characterized to be DPD−Cu(II) complexes.

Besides elemental analyses data verifying the 1:1 coordination stoichiometry in the solid state, Job's experiments using UV−vis spectroscopy were also performed to explore the coordination stoichiometry between CD/DPD and metal cations in aqueous solutions. As can be seen in Figure 1a, the Job's plot of the **1**/Ni(II) system showed a maximum at a molar fraction of 0.5 corresponding to a 1:1 **1**/Ni(II) coordination. The **2**/Ni(II) and **3**/Cu(II) systems also exhibited the same 1:1 coordination stoichiometry between CD/DPD complexes and metal cations. Because these stoichiometry values are very important for deducing structural features of polypseudorotaxanes **4**−**6**, we performed conductivity titration experiments to verify these values because the conductivity of the system always decreased upon complex formation. All of the Job's plots and mole ratio plots for CD/DPD−metal systems displayed a minimum at a concentration ratio of 1.0 (as exemplified in Figure 1b), which subsequently validated the accuracy of these values.

Conformation Analyses of Complexes 1−**3.** The understanding of the structural features of complexes **1**−**3** is very important for investigating their assembly behaviors. It is well-known that the elucidation of a crystal structure is one of the most convincing methods of unequivocally illustrating the geometrical conformation of CD derivatives. Unfortunately, even after our repeated attempts, only complex **2** produced a single crystal suitable for X-ray crystallography.[13] Therefore, we tried to elucidate conformations of complexes **1**−**3** through a combinational analysis based on circular dichroism and NMR spectroscopy. It has been amply

(14) Shukla, A. D.; Bajaj, H. C.; Das, A. *Angew. Chem., Int. Ed.* **2001**, *40*, 446.
(15) Kawaguchi, Y.; Harada, A. *Org. Lett.* **2000**, *2*, 1353.
(16) Wylie, R. S.; Macartney, D. H. *J. Am. Chem. Soc.* **1992**, *114*, 3136.

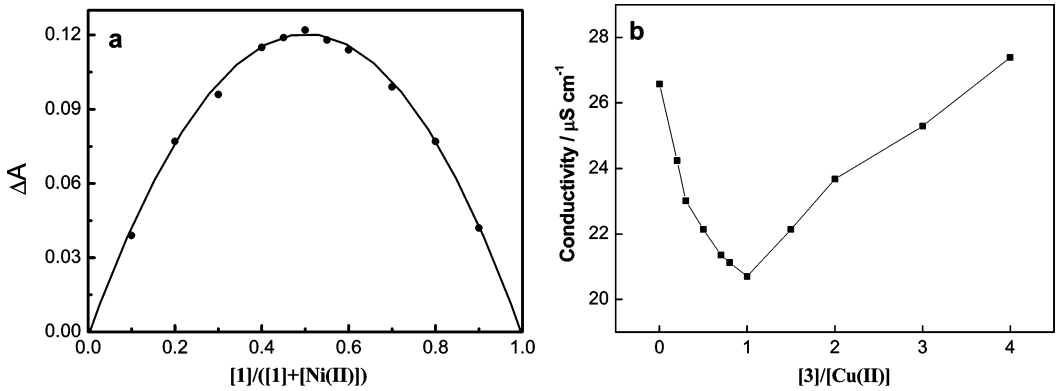

Figure 1. (a) A Job plot of the **1**/Ni(II) system at 25 °C in an aqueous solution {[**1**] + [Ni(II)] = 1.0 × 10^{-4} mol dm^{-3}; counteranion, Cl^{-1}}. (b) The dependence of the conductivity of $CuCl_2 \cdot 6H_2O$ (2.0 × 10^{-5} mol dm^{-3}) on the concentration of complex **3** (0.4, 0.6, 1.0, 1.4, 1.6, 1.8, 2.0, 3.0, 4.0, 6.0, and 8.0 × 10^{-5} mol dm^{-3}) at 25 °C in an aqueous solution.

demonstrated that the inclusion of a chromophoric achiral guest or moiety in a chiral host such as CDs produces induced circular dichroism (ICD) signals around their corresponding transition bands,[17] and the sign of ICD signals depends on the orientation of the guest transition moment relative to the CD axis.[18] That is, if the guest molecule is located inside the CD cavity, its electronic transition parallel to the CD axis gives a positive ICD signal, whereas the perpendicular transition gives a negative signal, but this situation is reversed for a guest located outside the CD cavity. Moreover, two-dimensional NMR spectroscopy is also an essential method in the study of the interaction between host and guest,[19] because one can conclude that two protons are closely located in space if NOE cross-peaks are detected between relevant protons in the NOESY or ROESY spectrum, and relative intensities of these cross-peaks depend on distances between corresponding protons. For CD-containing systems, if the guest molecule is included in the CD cavity, NOE correlations between guest's protons and CD's interior protons (H3/H5 protons) should be observed. According to the relative intensities of these correlations, one can estimate the orientation of the guest molecule within the CD cavity. Therefore, to deduce the conformation of complexes **1**−**3**, their circular dichroism spectra were measured at 25 °C in an aqueous solution.

As can be seen from Figure 2, complexes **1**−**3** displayed different ICD signals. The circular dichroism spectrum of **2** showed a positive Cotton-effect peak at 241 nm ($\Delta\epsilon = 0.70$ dm^{-3} mol^{-1} cm^{-1}) and a negative Cotton-effect peak at 269 nm ($\Delta\epsilon = -0.23$ dm^{-3} mol^{-1} cm^{-1}). Our preliminary work demonstrated that the DPD molecule penetrated the CD cavity with a slightly acclivitous orientation (Figure 3b).[13] According to this conformation, the DPD's transition moment (L) could be equivalently divided to two transition moments,

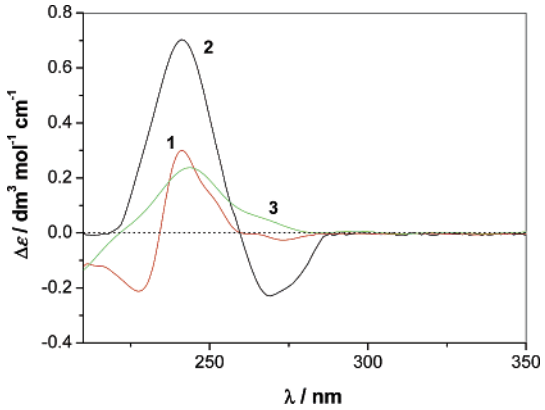

Figure 2. Circular dichroism spectra of CD/DPD complexes **1**−**3** in aqueous solutions at 25 °C.

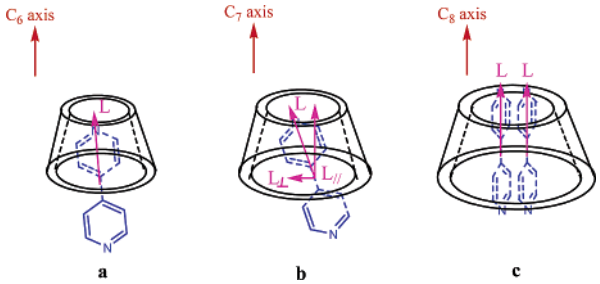

Figure 3. Possible conformations of complexes **1**−**3**.

one parallel ($L_{||}$) and the other perpendicular ($L_{\perp}$) to the CD axis, which respectively resulted in the positive and negative Cotton-effect peaks in the circular dichroism spectrum. In addition, considering the relatively small acclivitous angle between the DPD's transition moment (L) and the CD axis, we deduced that $L_{||}$ should be stronger than $L_{\perp}$, which consequently rationalized the stronger positive ICD of **2**.

Similarly, the circular dichroism spectrum of **1** also showed a positive Cotton-effect peak at 241 nm ($\Delta\epsilon = 0.30$ dm^{-3} mol^{-1} cm^{-1}) and a negative Cotton-effect peak at 274 nm ($\Delta\epsilon = -0.03$ dm^{-3} mol^{-1} cm^{-1}). This indicated that the DPD moiety in complex **1** might also adopt a tilt-in conformation upon inclusion complexation with the CD cavity similar to the case of **2**. Moreover, the higher ratio between intensities of the positive and negative Cotton-effect peaks for **1** ($I_+/I_- = 10$) than that for **2** ($I_+/I_- = 3$) indicated that the acclivitous angle between the DPD's transition

(17) (a) Connors, K. A. *Chem. Rev.* **1997**, *97*, 1325. (b) Rekharsky, M. V.; Inoue, Y. *Chem. Rev.* **1998**, *98*, 1875. (c) Zhdanov, Y. A.; Alekseev, Y. E.; Kompantseva, E. V.; Vergeichik, E. N. *Russ. Chem. Rev.* **1992**, *61*, 563.

(18) (a) Kajtár, M.; Horvath-Toro, C.; Kuthi, E.; Szejtli, J. *Acta Chim. Acad. Sci. Hung.* **1982**, *110*, 327. (b) Harata, K.; Uedaira, H. *Bull. Chem. Soc. Jpn.* **1975**, *48*, 375. (c) Zhang, X.; Nau, W. M. *Angew. Chem., Int. Ed.* **2000**, *39*, 544.

(19) Schneider, H.-J.; Hacker, F.; Rüdiger, V.; Ikeda, H. *Chem. Rev.* **1998**, *98*, 1755.

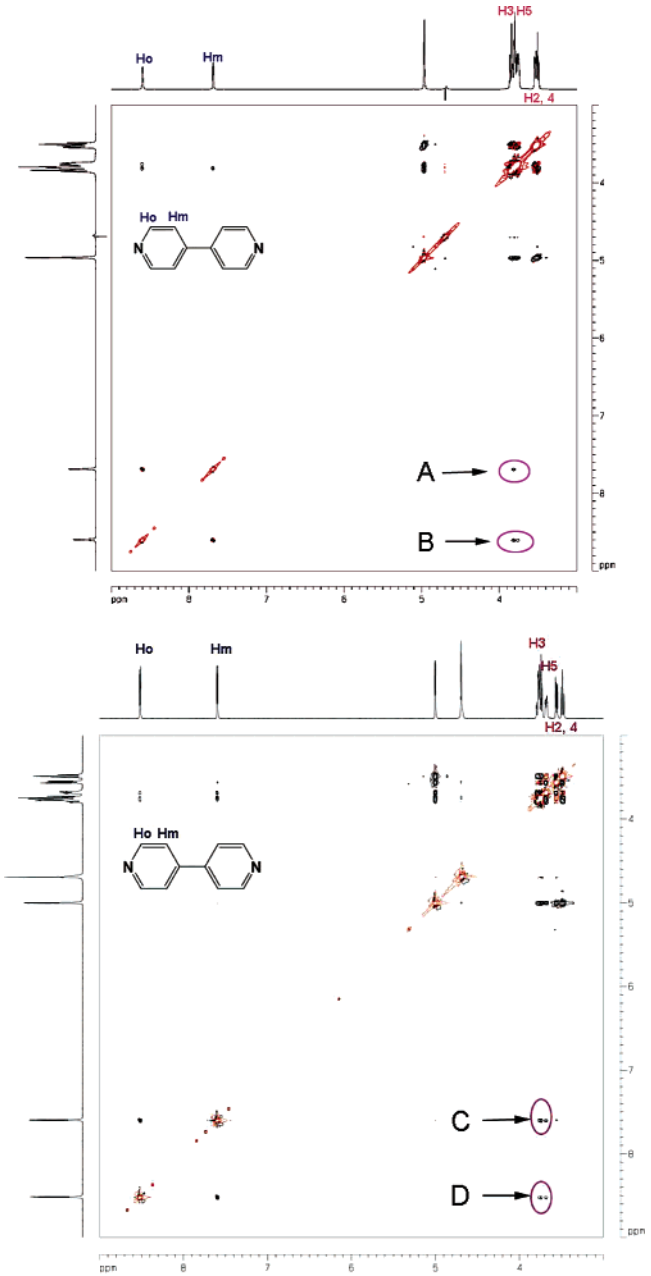

Figure 4. ROESY spectra of (a) **1** and (b) **3** in D_2O with a mixing time of 200 ms.

moment (L) and the CD axis in **1** was smaller than that in **2**. However, the appearance of a negative Cotton-effect peak at 228 nm ($\Delta\epsilon = -0.21$ dm^{-3} mol^{-1} cm^{-1}) indicated that the inclusion complexation mode of **1** was different from that of **2** to some extent. As seen from the ROESY spectrum of **1** (Figure 4a), CD's H3 protons gave strong NOE correlations (peak A) with DPD's ortho (H_o) and meta (H_m) protons, while CD's H5 protons only gave weak NOE correlations (peak B) with DPD's H_o protons. Considering that H3 protons are located near the secondary rim of the CD cavity, while H5 protons are near the primary rim, we deduced a possible conformation of **1**, as illustrated in Figure 3a. That is, one pyridine ring of DPD was included in the CD cavity from the secondary rim of the CD cavity, while the other was located outside. According to this conformation, the included pyridine ring gave a strong positive and a weak negative Cotton-effect peak, as described above, and the outside pyridine ring would produce a strong negative and a weak positive Cotton-effect peak (this positive peak may overlap with the strong positive peak at 241 nm). Because the included guest moiety was widely demonstrated to be more stable than the free one, Cotton-effect peaks assigned to the included pyridine ring appeared at a longer wavelength (241 nm) than those assigned to the free pyridine moiety (228 nm). Interestingly, the circular dichroism spectrum of **3** only showed a broad positive Cotton-effect peak at 244 nm ($\Delta\epsilon = 0.24$ dm^{-3} mol^{-1} cm^{-1}), indicating that two DPD molecules were accommodated in the γ-CD cavity with an orientation parallel to the CD axis. Because of the possible $\pi-\pi$ interactions between two DPD molecules, the Cotton-effect peak of **3** showed obvious broadening and an appreciable bathochromic shift (3 nm) as compared with the corresponding peaks of **1** and **2**. In the ROESY spectrum of **3** (Figure 4b), strong NOE correlations (peak C) between CD's H3/H5 protons and DPD's H_m protons, as well as relatively weak NOE correlations (peak D) between CD's H3/H5 protons and DPD's H_o protons, indicated that DPD molecules were deeply included in the CD cavity (Figure 3c). This conformation was further verified by a Corey−Pauling−Kultun molecular model study, showing that two DPD molecules could be well-accommodated in a γ-CD cavity.

TG-DTA Analyses. To investigate the thermal stabilities of **1**−**6**, their TG and DTA curves (see the Supporting Information) were recorded with a RIGAKU Standard-type spectrometer. Interestingly, the DTA curve of complex **1** displayed an endothermic peak at 228 °C. Similarly, the DTA curve of complex **2** also showed an endothermic peak at 244 °C.[13] In the control experiments, none of the α-, β-, and γ-CDs showed any thermic peak in the range of 100−300 °C. Therefore, we deduced that these endothermic peaks should correspond to the dissociation of the CD cavity with the included DPD. More interestingly, the DTA curve of complex **3** even showed two endothermic peaks at 249 and 267 °C. Because complex **3** possessed two DPD units accommodated in a γ-CD cavity, we deduced that these two peaks might correspond to the dissociation of the first and second DPDs from the γ-CD cavity. By comparing the temperatures for the dissociation of DPD from CD cavities, we deduced that the thermal stability of CD/DPD complexes increased with the enlargement of the CD cavity. However, these endothermic peaks disappeared in the DTA curves of **4**−**6**, indicating that the introduction of metal cations further stabilized the complexation of DPD with the CD cavity. At a higher temperature over 280 °C, all of the TG curves of **1**−**6** exhibited the obvious weight loss assigned to the decomposition of CD units. From these data, we could conclude that complexes **1**−**3** would dissociate to their parent components (CD and DPD) only at a temperature above 220 °C, and polypseudorotaxanes **4**−**6** never dissociated before the decomposition of the CD unit, which jointly indicated that complexes **1**−**3** and polypseudorotaxanes **4**−**6** were fairly stable from a thermal viewpoint.

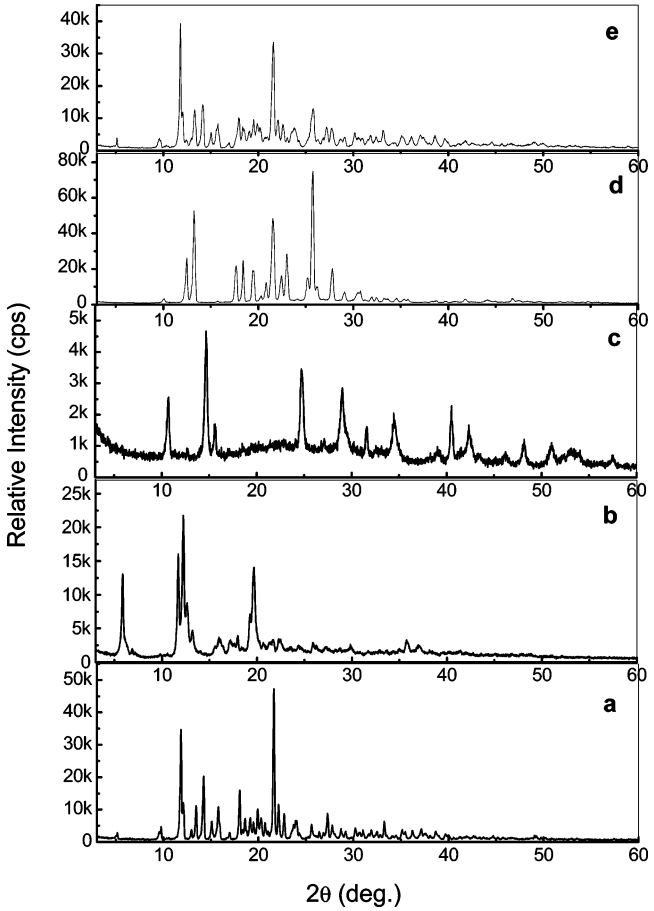

Figure 5. X-ray powder diffraction patterns of (a) α-CD, (b) complex **1**, (c) polypseudorotaxane **4**, (d) free DPD, and (e) a physical mixture of α-CD and DPD.

Powder X-ray Diffraction. Powder X-ray diffraction (XRD) is a generally used method to characterize CD-based complexes and aggregates because XRD patterns of the resulting complexes and aggregates should be different from those of native CDs.[6g,12a,20] On the basis of the XRD patterns of CDs and DPD (Figure 5a and b and in the Supporting Information), we could find that α-CD, β-CD, and DPD were in crystalline form, while γ-CD was somewhat amorphous. In the control experiments, the physical mixture of CD with DPD (molar ratio of 1:1 for α-CD/DPD and β-CD/DPD and 1:2 for γ-CD/DPD) showed a diffractogram that could be characterized as a superimposition of CD's and DPD's diffractograms. In contrast, the XRD patterns of complexes **1**−**3** exhibited appreciable differences from those of corresponding CD/DPD physical mixtures in terms of the peak shape, peak position, and relative intensity. We have demonstrated that the β-CD/DPD complex **2** gave a different diffractogram from that of a β-CD/DPD mixture, exhibiting appreciable shifts of characteristic reflections.[13] Herein, similar phenomena were also found in the cases of the α-CD/DPD and γ-CD/DPD systems. For example, the diffractogram of α-CD (Figure 5a) showed two characteristic reflections at $2\theta = 11.8°$ ($d = 7.47$ Å) and 12.1° ($d = 7.31$ Å), and that of DPD showed a characteristic reflection at

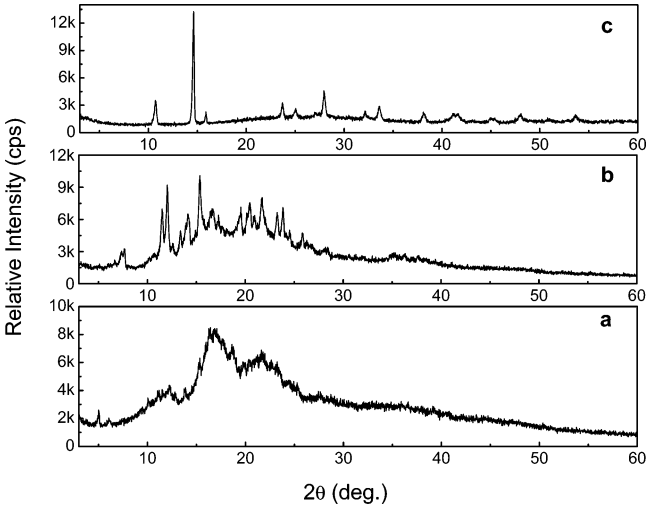

Figure 6. X-ray powder diffraction patterns of (a) γ-CD, (b) complex **3**, and (c) polypseudorotaxane **6**.

$2\theta = 12.5°$ ($d = 7.06$ Å) (see the Supporting Information). However, these characteristic reflections changed to $2\theta = 11.7°$ ($d = 7.56$ Å), 12.2° ($d = 7.23$ Å), and 12.6° ($d = 7.00$ Å) in the diffractogram of complex **1**. In addition, characteristic reflections of γ-CD and DPD, which appeared respectively at $2\theta = 12.3°$ ($d = 7.21$ Å) and 12.5° ($d = 7.06$ Å) in diffractograms of γ-CD and DPD, were changed to $2\theta = 12.0°$ ($d = 7.34$ Å) and 12.6° ($d = 7.03$ Å) in the diffractogram of complex **3**. These phenomena jointly indicated that new species, in this case, CD/DPD complexes, were formed between CD and DPD in the solid state, and the original arrangement mode of CD was changed after the introduction of DPD.

Interestingly, metallo-linked polypseudorotaxanes, especially polypseudorotaxanes **4** and **6**, gave obviously different XRD patterns from those of their precursors **1**−**3**, exhibiting a number of sharp reflections in their diffractograms (Figures 5 and 6 and in the Supporting Information). These indicated that the coordination of metal cations not only reoriented the CD/DPD units upon construction but also enabled an ordered structure of the resulting polypseudorotaxane with an arrangement mode different from that of its precursor CD/DPD complex.

Scanning Electron Microscope. To explore the morphology of complexes **1**−**3** and polypseudorotaxanes **4**−**6** in the solid state, their SEM images were recorded (Figure S8 in the Supporting Information). A comparison of these SEM images revealed that the apparent conformations of polypseudorotaxanes **4**−**6** were distinct from those of complexes **1**−**3**. For example, all of the CD/DPD complexes **1**−**3** displayed a sheetlike morphology. However, polypseudorotaxanes **4**−**6** could be characterized as having a regular rodlike (for **4**) or square-pillarlike (for **5** and **6**) morphology. These phenomena, together with the XRD results, jointly indicated that CD/DPD complexes would convert to a more ordered structure in the solid state after coordination with metal cations.

Transmission Electron Microscope. TEM has become a convenient and widely employed method for the elucidation

(20) Harada, A.; Suzuki, S.; Okada, M.; Kamachi, M. *Macromolecules* **1996**, *29*, 5611.

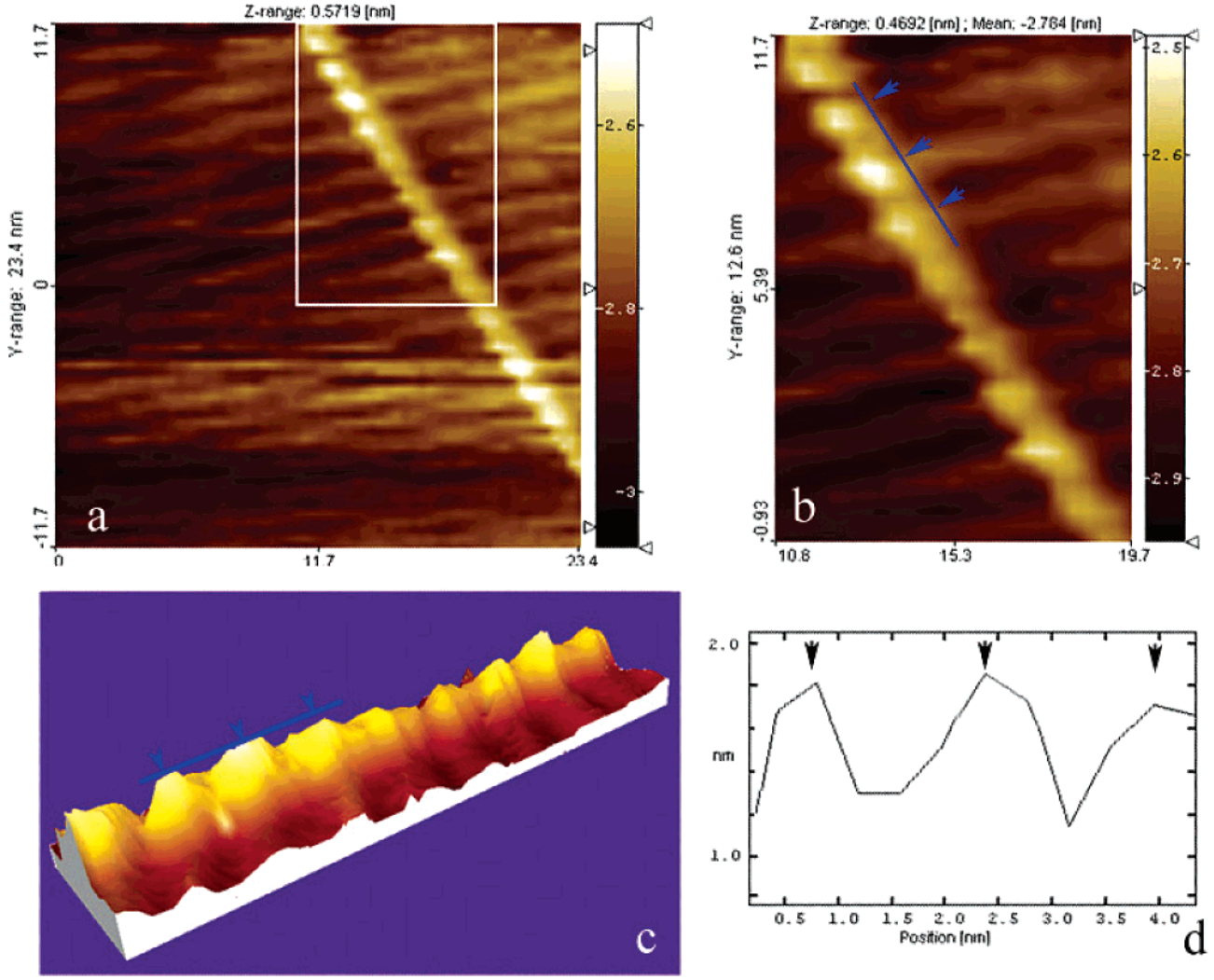

Figure 7. (a) STM image of polypseudorotaxane **6**. (b) Enlarged version of the image in part a. (c) 3D version of the image in part b. (d) Line profile of the image in parts b and c. *V* (bias), +100 mV; *I* (bias), 1.001 nA.

of the size and shape of polypseudorotaxanes.[21] To investigate the morphology of metallo-linked polypseudorotaxanes in solution, their TEM images were recorded at a concentration up to 1.0×10^{-4} M. From Figure S9 in the Supporting Information, we could see that polypseudorotaxanes **4**−**6** displayed a rodlike structure in solution. A further examination of high-resolution transmission electron microscopy (HR-TEM) images showed that each rodlike structure was composed of many linear nanostructures, but their boundaries were not very clear (Figure S9b and d in the Supporting Information). Therefore, these TEM images could only been used to measure the length of polypseudorotaxanes. The results showed that the average length of polypseudorotaxane **4** constructed by α-CD/DPD and Ni(II) was ca. 1600 nm, while that of polypseudorotaxane **6** formed by γ-CD/DPD and Cu(II) was ca. 200 nm, which indicated that ca. 1200 and 160 CD/DPD-metal units were joined together to form polypseudorotaxanes **4** and **6**, respectively. In a preliminary work, we reported that the length of the β-CD/DPD−Ni(II) polypseudorotaxane **5** was ca. 450 nm,[13] indicating the presence of ca. 400 β-CD/DPD−Ni(II) units in a polypseudorotaxane. Therefore, we can deduce that the average length of the polypseudorotaxane tended to increase with the enlargement of the CD cavity used. This concept will efficiently facilitate the design and synthesis of new supramolecular architectures with special size; although, its mechanism is still unknown.

Scanning Tunneling Microscope. TEM experiments demonstrated that polypseudorotaxanes **4**−**6** tended to form polymeric fibers at a relatively high concentration (1.0×10^{-4} M). To examine the morphology of individual polypseudorotaxanes, their STM images were recorded at a low concentration (5×10^{-6} M). For example, Figure 7 illustrates a typical STM image of polypseudorotaxane **6**. As can be seen from Figure 7, the STM image of **6** displayed a regular linear arrangement composed of many bright dots. A further measurement indicated that the width and height of each bright dot was ca. 1.6 and 1.8 nm, respectively, which was basically consistent with the external diameter of a γ-CD cavity (1.75 nm). Moreover, the average distance between two adjacent bright dots was 1.5 ± 0.1 nm, which was similar

(21) (a) Hamley, I. W. *Angew. Chem., Int. Ed.* **2003**, *42*, 1692. (b) van Bommel, K. J. C.; Friggeri, A.; Shinkai, S. *Angew. Chem., Int. Ed.* **2003**, *42*, 980.

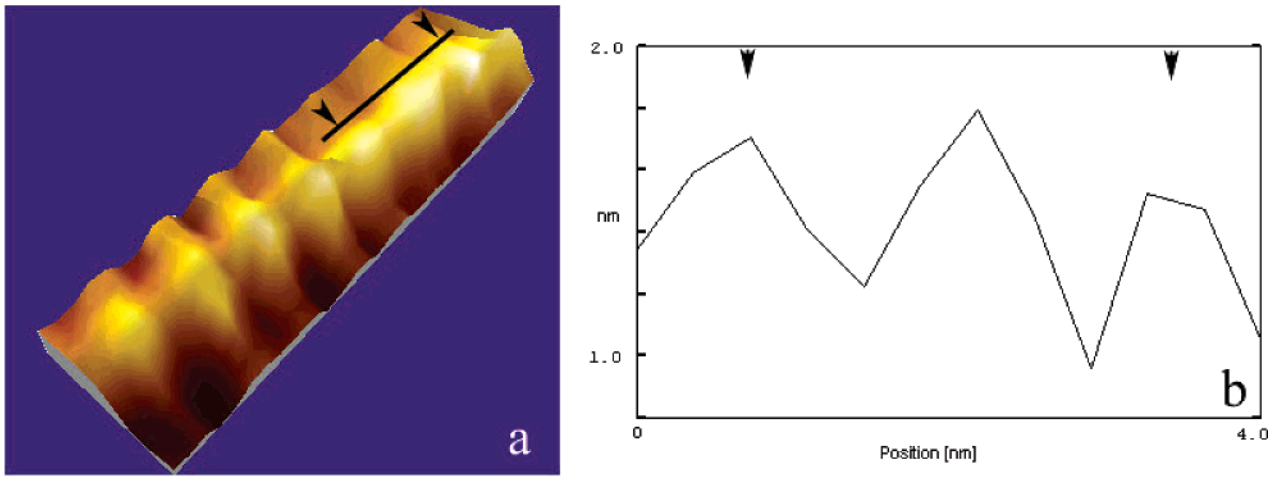

Figure 8. (a) STM image of polypseudorotaxane **4**. (b) Line profile of image in part a. *V* (bias), +100 mV; *I* (bias), 1.001 nA.

to the sum of the lengths of a DPD skeleton (0.86 nm, obtained by a MM2 calculation) and two Cu−N bonds (according to many reports about crystal structures of Cu−N complexes, an average Cu−N bond length is ca. 0.2 nm). According to this information, we assigned Figure 7c as follows: each bright dot corresponded to a γ-CD/DPD unit that lay on the highly oriented pyrrolytic graphite (HOPG) substrate with the γ-CD's C_8 axis parallel to the HOPG surface, and the copper(II) ion was located at the intersection between two adjacent bright dots. Similarly, the α-CD/DPD-based polypseudorotaxane **4** also showed a linear array on the HOPG surface. By comparing the average size of the bright dots in Figure 8a with the external diameter of an α-CD cavity (1.46 nm), we deduced that each bright dot (height, 1.7 nm; width, 1.5 nm) in the linear array should represent an α-CD/DPD unit. Moreover, the average distance between two bright dots was measured to be 1.4 ± 0.1 nm, which was almost identical to the sum of the lengths of a DPD skeleton (0.86 nm) and two Ni−N bonds (the generally reported Ni−N bond length is ca. 0.2 nm). In the preliminary work, we reported that the β-CD/DPD−Ni(II) polypseudorotaxane **5** also adopted a linear topology on the HOPG surface.[13] Therefore, we can draw a conclusion that these CD/DPD complexes formed supramolecular chains with a linear arrangement through the coordination linkage of metal cations. At an appropriate concentration ($\geq 1.0 \times 10^{-4}$ M), these supramolecular chains would spontaneously assemble to bunchy fibers. In each supramolecular chain, the presence of many coordinated DPD−metal pairs might enable the supramolecular chain to transport the charge or energy within the chain, and the presence of numerous CD cavities would efficiently insulate the adjacent supramolecular chains in a fiber. Therefore, these CD/DPD−metal chains might have a potential application as nanometer-scaled molecular cables.[10] Endeavors to explore the application of these supramolecules are currently in progress.

Conclusion

In summary, we successfully prepared a series of inclusion complexes of α-, β-, and γ-CDs with 4,4′-dipyridine and comprehensively investigated their assembly behaviors in the presence of transition-metal ions. The results show that the volume of the CD used not only determines the inclusion complexation stoichiometry between the CD and 4,4′-dipyridine but also predominates the morphology of the resulting polypseudorotaxanes. That is, the length of the resulting polypseudorotaxane decreases with the enlargement of the CD cavity. This approach using simple CD inclusion complexes and metal cations to construct nanometer-scaled functional molecular assemblies may provide a convenient means for designing novel functional materials, which possess the potential to serve as molecular devices and molecular machines.

Acknowledgment. We are grateful to the National Natural Science Foundation (No. 90306009, 20402008, 20421202, and 20572052) for financial support.

Supporting Information Available: ^{1}H NMR spectra of DPD and complexes **1**−**3**; XRD patterns of β-CD, complex **2**, and polypseudorotaxane **5**; TG-DTA curves of CDs, complexes **1**−**3**, and polypseudorotaxanes **4**−**6**; SEM images of complexes **1**−**3** and polypseudorotaxanes **4**−**6**; and TEM images of **4** and **6**. This material is available free of charge via the Internet at http://pubs.acs.org.

IC0601438